LA-UR-21-28181
Approved for public release; distribution is unlimited.

Title: Verification of Combined VR Techniques, Derivation of Future Time Equation, and Integration of LLNL Pulsed Sphere V&V Suite

Author(s): Pearson, Eric John

Intended for: Report

Issued: 2021-08-16

Verification of Combined VR Techniques, Derivation of Future Time Equation, and Integration of LLNL Pulsed Sphere V&V Suite

Eric Pearson
Monte Carlo Codes Group (XCP-3)

Lab Mentors: Joel Kulesza & Jennifer Alwin

August 11, 2021

Los Alamos NATIONAL LABORATORY EST. 1943

NNSA National Nuclear Security Administration

Managed by Triad National Security, LLC for the U.S. Department of Energy's NNSA

Acknowledgments

- The verification of the combined variance-reduction techniques would not have been possible without prior researchers in the field establishing the history score moment formalism and its application to variance-reduction techniques [1–4]
- The derivation of the future time equation was funded in part by the Consortium for Monitoring, Technology, and Verification under Department of Energy National Nuclear Security Administration award number DE-NA0003920 and performed with the guidance of Prof. Brian Kiedrowski of the University of Michigan
- The addition of the LLNL pulsed sphere benchmarks to the verification and validation suite was greatly aided by prior work. Input files were originally developed by others at LANL [5, 6] and the verification and validation framework was developed by Mike Rising, Colin Josey, and Joel Kulesza of XCP-3

Presentation Overview

Proof that Combining Forced Collisions with DXTRAN Produces an Unbiased Simulation

Background: Forced-Collision Technique

- Goal: Sample more collisions in certain cells
- Technique: Split particles into collided and transmitted parts
  - Collided particle undergoes a collision in the cell
  - Transmitted particle streams through the cell

$$w_t(\boldsymbol{p}) = w_0 \exp(-\ell(\boldsymbol{x}, \boldsymbol{x}_s(\boldsymbol{x}, \hat{\boldsymbol{\Omega}}))), \tag{1}$$

$$w_c(\boldsymbol{p}) = w_0 - w_t(\boldsymbol{p}) = w_0 \Big(1 - \exp(-\ell(\boldsymbol{x}, \boldsymbol{x}_s(\boldsymbol{x}, \hat{\boldsymbol{\Omega}})))\Big), \tag{2}$$

$$\ell(\boldsymbol{x}, \boldsymbol{x}') \equiv \int_0^{\|\boldsymbol{x}'-\boldsymbol{x}\|} \Sigma_t\left(\boldsymbol{x} + a\frac{\boldsymbol{x}'-\boldsymbol{x}}{\|\boldsymbol{x}'-\boldsymbol{x}\|}\right) da \tag{3}$$

- For this work, only one forced collision when entering a cell

Diagram: Forced-Collision Technique

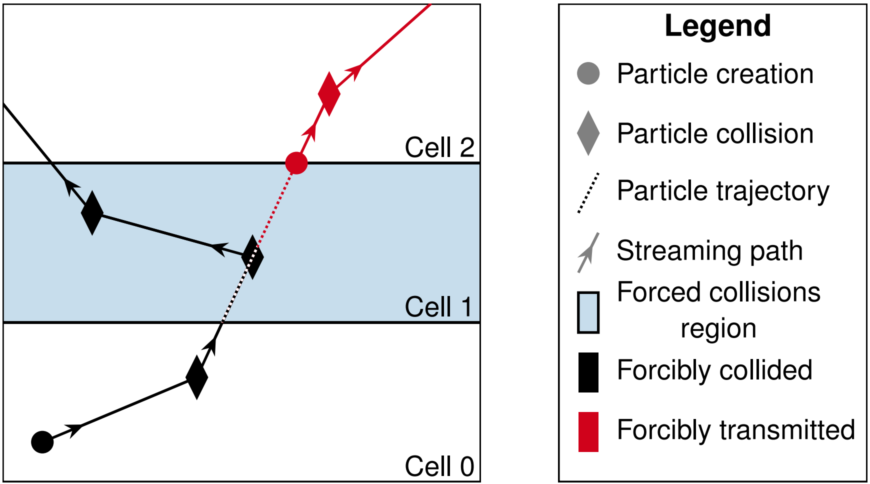

Background: DXTRAN Technique

- Goal: Sample more random walks in a region
- Technique: Following source or collision, split particle into DXTRAN and non-DXTRAN parts
  - DXTRAN particle is created on the surface of the DXTRAN region
  - Non-DXTRAN particle is killed if it tries to enter the DXTRAN region

$$w_{DX}(\boldsymbol{p}) = w_0 \frac{f(\boldsymbol{x}, \hat{\boldsymbol{\Omega}} \to \hat{\boldsymbol{\Omega}}', E \to E')}{f_{DX}(\boldsymbol{x}, \hat{\boldsymbol{\Omega}} \to \hat{\boldsymbol{\Omega}}', E \to E')} \exp(-\ell(\boldsymbol{x}, \boldsymbol{x}_{DX}(\boldsymbol{x}, \hat{\boldsymbol{\Omega}}'))) \tag{4}$$

- For this work, one spherical region without weight cutoff, DXC, or DD

Diagram: DXTRAN Technique

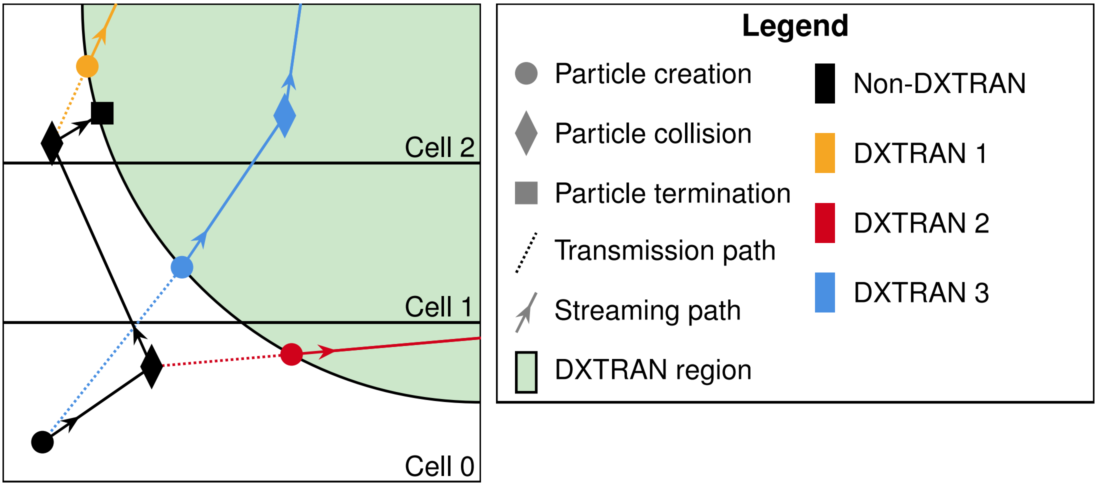

Background: Combined Techniques

- Goal: Sample more collisions in certain cells and more random walks in another, possibly overlapping, region
- Technique: Implemented as before with two exceptions
  - Collisions are forced before reaching the DXTRAN region
  - Forcibly transmitted particle is killed if it intersects the DXTRAN region
- Matches what is done in the MCNP® code

Diagram: Combined Techniques

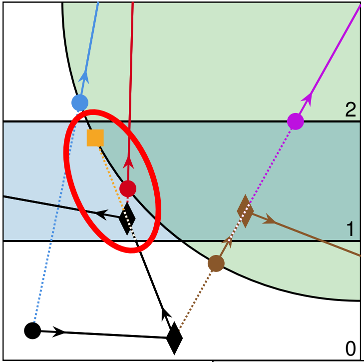

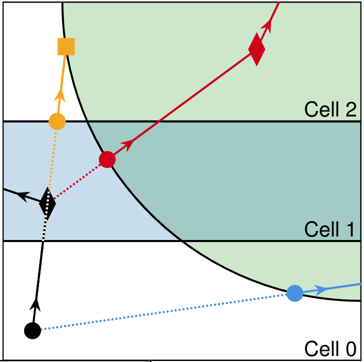

Legend

Particle creation	Non-DXTRAN, forcibly collided
Particle collision	Non-DXTRAN, forcibly transmitted
Particle termination	DXTRAN, forcibly collided
Transmission path	DXTRAN, forcibly transmitted
Streaming path	DXTRAN, unforced 1
Forced Collisions	DXTRAN, unforced 2
DXTRAN	

Motivation for This Work

MCNP Issue #53227

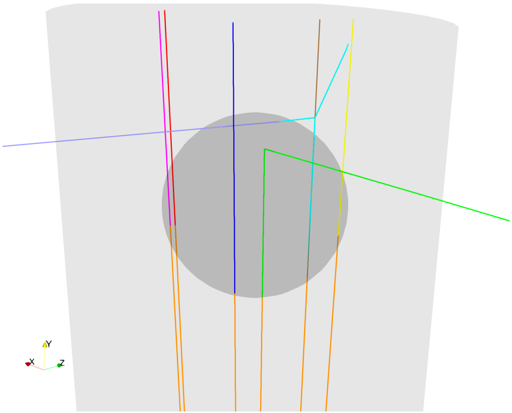

- Prompted by unexplained behavior
- Provide theoretical justification for:
  - Forced-collision technique
  - DXTRAN technique
  - Both techniques combined
- Provide insight into what effect these techniques have on transport

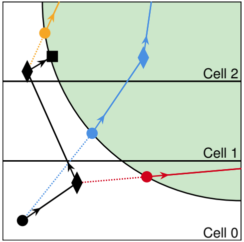

Approach to This Work

- Form the History Score Probability Density Functions (HSPDFs)
  - Sum of all disjoint random-walk steps
  - Written in integral form with operator notation
- Calculation the History Score Moment Equations (HSMEs)
  - First score moment of HSPDFs
- Show that HSMEs with VR in play reduces to the analog HSME
  - Convert HSMEs into characteristic coordinates and manipulate
- Throughout phase space is position, angle, energy, and weight

$$\boldsymbol{p} \equiv (\boldsymbol{x}, \hat{\boldsymbol{\Omega}}, E, w)$$

- Non-multiplying media is assumed

Analog Simulation: HSPDF

- HSPDF governs the probability of a history starting at $\boldsymbol{p}$ contributing ds about s

$$\begin{aligned}\psi_0(\boldsymbol{p}, s)ds = &\mathcal{T}(\boldsymbol{p}, \boldsymbol{p}_1)\mathcal{K}_A(\boldsymbol{p}_1, \boldsymbol{p}_2)\int f_A(\boldsymbol{p}_1, s_A)\delta(s - s_A)ds_A ds \\ &+ \mathcal{T}(\boldsymbol{p}, \boldsymbol{p}_1)\mathcal{K}_E(\boldsymbol{p}_1, \boldsymbol{p}_3)\int f_E(\boldsymbol{p}_1, s_E)\psi_0(\boldsymbol{p}_3, s - s_E)ds_E ds \\ &+ \mathcal{T}(\boldsymbol{p}, \boldsymbol{p}_4)\mathcal{S}(\boldsymbol{p}_4, \boldsymbol{p}_5)\int f_S(\boldsymbol{p}_4, s_S)\psi_0(\boldsymbol{p}_5, s - s_S)ds_S ds\end{aligned} \tag{5}$$

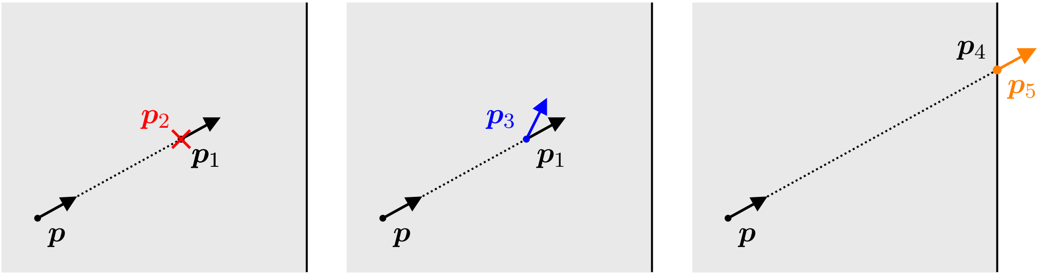

Analog Simulation: HSME

- HSME is the first score moment of the HSPDF

$$\Psi_0(\boldsymbol{p}) = \int s\psi_0(\boldsymbol{p}, s)ds \tag{6}$$

- The expected value is taken from the score PDF

$$\bar{s}_e(\boldsymbol{p}) = \int s f_e(\boldsymbol{p}, s)ds \tag{7}$$

- HSME governs the expected score from a history at $\boldsymbol{p}$

$$\begin{aligned}\Psi_0(\boldsymbol{p}) = \; & \mathcal{T}(\boldsymbol{p}, \boldsymbol{p}_1)\mathcal{K}_A(\boldsymbol{p}_1, \boldsymbol{p}_2)\bar{s}_A(\boldsymbol{p}_1) \\ & + \mathcal{T}(\boldsymbol{p}, \boldsymbol{p}_1)\mathcal{K}_E(\boldsymbol{p}_1, \boldsymbol{p}_3)(\bar{s}_E(\boldsymbol{p}_1) + \Psi_0(\boldsymbol{p}_3)) \\ & + \mathcal{T}(\boldsymbol{p}, \boldsymbol{p}_4)\mathcal{S}(\boldsymbol{p}_4, \boldsymbol{p}_5)(\bar{s}_S(\boldsymbol{p}_4) + \Psi_0(\boldsymbol{p}_5))\end{aligned} \tag{8}$$

Analog Simulation: Characteristic Coordinates

- Operators are defined in terms of characteristic coordinates
- Characteristic coordinate form of HSME
  - Found from expanding operator definitions
  - Less compact than operator form
  - Allows direct comparison between HSMEs

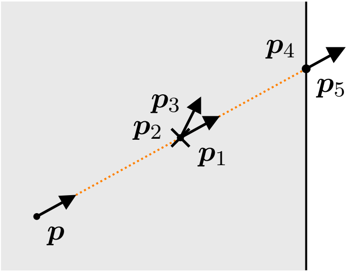

$$
\begin{aligned}
\Psi_0(\boldsymbol{p}) = \int_0^{a_S(\boldsymbol{x},\hat{\boldsymbol{\Omega}})} & \exp(-\ell(\boldsymbol{x}, \boldsymbol{x} + a\hat{\boldsymbol{\Omega}})) \\
& \times \Bigg(\Sigma_a(\boldsymbol{x} + a\hat{\boldsymbol{\Omega}}, E)\bar{s}_A(\boldsymbol{x} + a\hat{\boldsymbol{\Omega}}, \hat{\boldsymbol{\Omega}}, E) \\
& + \iint \Sigma_s(\boldsymbol{x} + a\hat{\boldsymbol{\Omega}}, \hat{\boldsymbol{\Omega}} \to \hat{\boldsymbol{\Omega}}_3, E \to E_3) \\
& \quad \times \left(\bar{s}_E(\boldsymbol{x} + a\hat{\boldsymbol{\Omega}}, \hat{\boldsymbol{\Omega}}, E) + \Psi_0(\boldsymbol{x} + a\hat{\boldsymbol{\Omega}}, \hat{\boldsymbol{\Omega}}_3, E_3, w) \right) \Bigg) d\Omega_3 dE_3 da \\
& + \exp(-\ell(\boldsymbol{x}, \boldsymbol{x} + a_S(\boldsymbol{x}, \hat{\boldsymbol{\Omega}})\hat{\boldsymbol{\Omega}})) \\
& \times \left(\bar{s}_S(\boldsymbol{x} + a_S(\boldsymbol{x}, \hat{\boldsymbol{\Omega}})\hat{\boldsymbol{\Omega}}, \hat{\boldsymbol{\Omega}}, E) + \Psi_0(\boldsymbol{x} + a_S(\boldsymbol{x}, \hat{\boldsymbol{\Omega}})\hat{\boldsymbol{\Omega}}, \hat{\boldsymbol{\Omega}}, E, w) \right)
\end{aligned} \tag{9}
$$

Forced Collisions: Governing Equation

- The forced-collision HSME has only two possible random-walk steps
  - Each step will have both a collision and a transmission
  - Collision is either absorptive or emissive
  - If no collisions are forced, HSME looks like analog

$$
\begin{aligned}
\Psi_{FC}(\boldsymbol{p}) = \mathcal{B}_c(\boldsymbol{p},\boldsymbol{p}_1)\mathcal{K}_A(\boldsymbol{p}_1,\boldsymbol{p}_2) \\
\times\left(\bar{s}_A(\boldsymbol{p}_1) + \mathcal{B}_t(\boldsymbol{p},\boldsymbol{p}_4)\mathcal{S}(\boldsymbol{p}_4,\boldsymbol{p}_5)(\bar{s}_S(\boldsymbol{p}_4) + \Psi_{FC}(\boldsymbol{p}_5))\right) \\
+ \mathcal{B}_c(\boldsymbol{p},\boldsymbol{p}_1)\mathcal{K}_E(\boldsymbol{p}_1,\boldsymbol{p}_3) \\
\times\left(\bar{s}_E(\boldsymbol{p}_1) + \Psi^0_{FC}(\boldsymbol{p}_3) + \mathcal{B}_t(\boldsymbol{p},\boldsymbol{p}_4)\mathcal{S}(\boldsymbol{p}_{4,}\boldsymbol{p}_5)(\bar{s}_S(\boldsymbol{p}_4) + \Psi_{FC}(\boldsymbol{p}_5))\right), \\
\boldsymbol{p} \in \{\boldsymbol{p}_{FC}\}
\end{aligned} \tag{10}
$$

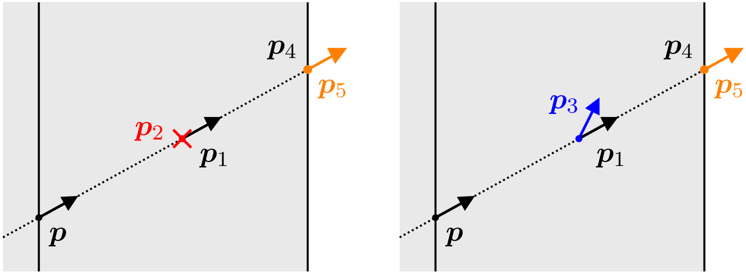

Forced Collisions: Equivalence to Analog Transport

- Can be rewritten as

$$\begin{aligned}\Psi_{FC}(\boldsymbol{p}) = {} & \mathcal{B}_c(\boldsymbol{p},\boldsymbol{p}_1)\mathcal{K}_A(\boldsymbol{p}_1,\boldsymbol{p}_2)\bar{s}_A(\boldsymbol{p}_1) \\ & + \mathcal{B}_c(\boldsymbol{p},\boldsymbol{p}_1)\mathcal{K}_E(\boldsymbol{p}_1,\boldsymbol{p}_3)\big(\bar{s}_E(\boldsymbol{p}_1) + \Psi^0_{FC}(\boldsymbol{p}_3)\big) \\ & + \mathcal{B}_c(\boldsymbol{p},\boldsymbol{p}_1)(\mathcal{K}_A(\boldsymbol{p}_1,\boldsymbol{p}_2) + \mathcal{K}_E(\boldsymbol{p}_1,\boldsymbol{p}_3)) \\ & \times \mathcal{B}_t(\boldsymbol{p},\boldsymbol{p}_4)\mathcal{S}(\boldsymbol{p}_{4,}\boldsymbol{p}_5)(\bar{s}_S(\boldsymbol{p}_4) + \Psi_{FC}(\boldsymbol{p}_5)),\ \boldsymbol{p} \in \{\boldsymbol{p}_{FC}\}\end{aligned} \tag{11}$$

- Sampling biased PDF with weight adjustment is equivalent to analog PDF

$$\mathcal{B}_c(\boldsymbol{p},\boldsymbol{p}_1) + w_c(\boldsymbol{p}) \to \mathcal{T}(\boldsymbol{p},\boldsymbol{p}_1)$$

$$\mathcal{B}_t(\boldsymbol{p},\boldsymbol{p}_4) + w_t(\boldsymbol{p}) \to \mathcal{T}(\boldsymbol{p},\boldsymbol{p}_4)$$

- Following both forced collisions means it's going to happen

$$\mathcal{B}_c(\boldsymbol{p},\boldsymbol{p}_1)(\mathcal{K}_A(\boldsymbol{p}_1,\boldsymbol{p}_2) + \mathcal{K}_E(\boldsymbol{p}_1,\boldsymbol{p}_3)) = 1$$

- **Applying to Eq. 11, turns into Eq. 8**

$$\boldsymbol{\Psi_{FC}(p),\ p \in \{p_{FC}\} = \Psi_0(p)}$$

DXTRAN: Governing Equation

- The DXTRAN HSME looks like the analog HSME with an extra branch

$$\begin{aligned}\Psi_{DX}(\boldsymbol{p}) = {} & \mathcal{T}_{DX}(\boldsymbol{p},\boldsymbol{p}_1)\mathcal{K}_A(\boldsymbol{p}_1,\boldsymbol{p}_2)\bar{s}_A(\boldsymbol{p}_1) \\ & + \mathcal{T}_{DX}(\boldsymbol{p},\boldsymbol{p}_1)\mathcal{K}_E(\boldsymbol{p}_1,\boldsymbol{p}_3)(\bar{s}_E(\boldsymbol{p}_1) + \Psi_{DX}(\boldsymbol{p}_3)) \\ & + \mathcal{T}_{DX}(\boldsymbol{p},\boldsymbol{p}_4)\mathcal{S}(\boldsymbol{p}_4,\boldsymbol{p}_5)(\bar{s}_S(\boldsymbol{p}_4) + \Psi_{DX}(\boldsymbol{p}_5)) \\ & + \mathcal{T}_{DX}(\boldsymbol{p},\boldsymbol{p}_1)\mathcal{K}_E(\boldsymbol{p}_1,\boldsymbol{p}_3)\mathcal{B}_{DX}(\boldsymbol{p}_1,\boldsymbol{p}_6)\Psi_{DX}(\boldsymbol{p}_6)\end{aligned} \tag{12}$$

- Differences between Eq. 12 and Eq. 8
  - $\mathcal{T}_{DX}$ kills particles attempting to enter the DXTRAN region
  - $\mathcal{B}_{DX}$ creates a DXTRAN particle following source/collision events

DXTRAN: α/β Form

- Need to break HSME into two recursively interdependent equations
  - α form governs transport only where DXTRAN particles are created
  - β form governs transport elsewhere
  - α/β form is exactly equivalent to previous form of HSMEs
  - α/β notation is unique to this work

$$\begin{aligned}\Psi^{\alpha}_{DX}(\boldsymbol{p}) = \int f(\boldsymbol{x}, \hat{\boldsymbol{\Omega}} \to \hat{\boldsymbol{\Omega}}_1, E \to E_1)\Psi^{\beta}_{DX}(\boldsymbol{p}_1)\delta(\boldsymbol{x}_1 - \boldsymbol{x})\delta(w_1 - w)d\boldsymbol{p}_1 \\ + \mathcal{B}_{DX}(\boldsymbol{p}, \boldsymbol{p}_2)\Psi^{\beta}_{DX}(\boldsymbol{p}_2)\end{aligned} \tag{13}$$

and

$$\begin{aligned}\Psi^{\beta}_{DX}(\boldsymbol{p}) &= \mathcal{T}_{DX}(\boldsymbol{p}, \boldsymbol{p}_1)\mathcal{K}_A(\boldsymbol{p}_1, \boldsymbol{p}_2)\bar{s}_A(\boldsymbol{p}_1) \\ &+ \mathcal{T}_{DX}(\boldsymbol{p}, \boldsymbol{p}_1)\mathcal{K}'_E(\boldsymbol{p}_1, \boldsymbol{p}_3)(\bar{s}_E(\boldsymbol{p}_1) + \Psi^{\alpha}_{DX}(\boldsymbol{p}_3)) \\ &+ \mathcal{T}_{DX}(\boldsymbol{p}, \boldsymbol{p}_4)\mathcal{S}(\boldsymbol{p}_4, \boldsymbol{p}_5)\left(\bar{s}_S(\boldsymbol{p}_4) + \Psi^{\beta}_{DX}(\boldsymbol{p}_5)\right)\end{aligned} \tag{14}$$

- The analog HSME is also be cast into α/β form

DXTRAN: α Form

$$\Psi^{\alpha}_{DX}(\boldsymbol{p}) = \int f(\boldsymbol{x}, \hat{\boldsymbol{\Omega}} \to \hat{\boldsymbol{\Omega}}_1, E \to E_1)\Psi^{\beta}_{DX}(\boldsymbol{p}_1)\delta(\boldsymbol{x}_1 - \boldsymbol{x})\delta(w_1 - w)d\boldsymbol{p}_1 + \mathcal{B}_{DX}(\boldsymbol{p}, \boldsymbol{p}_2)\Psi^{\beta}_{DX}(\boldsymbol{p}_2)$$

- The α form consolidates DXTRAN and non-DXTRAN β transport

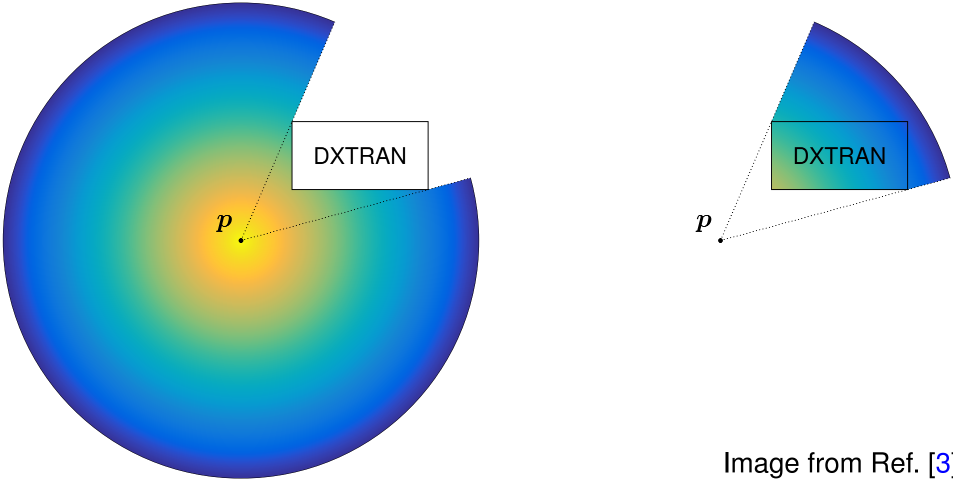

Image from Ref. [3]

DXTRAN: Approach to Show Equivalence

- Temporarily assume technique is only applied once
  - Once proven fair following emergence, assumption isn't needed
  - Allows subsequent $\Psi^{\alpha}_{DX} = \Psi^{\alpha}_{0}$
- Analyze all cases following emergence
  - Phase space is divided by angle and DXTRAN sphere
  - For all cases show technique is fair
- Technique is only unbiased following emergence

DXTRAN: Equivalence to Analog

- DXTRAN particle with weight adjustment is equivalent to analog

$$\mathcal{B}_{DX}(\boldsymbol{p}, \boldsymbol{p}') + w_{DX}(\boldsymbol{p}) \rightarrow \mathcal{T}(\boldsymbol{p}, \boldsymbol{p}')$$

- X_3: Won't be truncated
- $X_1 + X_4$: Truncation is compensated for by DXTRAN
- $X_2 + X_5$: Eventual truncation is compensated for by DXTRAN
- For all cases, DXTRAN transport is equivalent to analog following emergence

$$\boldsymbol{\Psi}^{\alpha}_{DX}(\boldsymbol{p}) = \boldsymbol{\Psi}^{\alpha}_{0}(\boldsymbol{p})$$

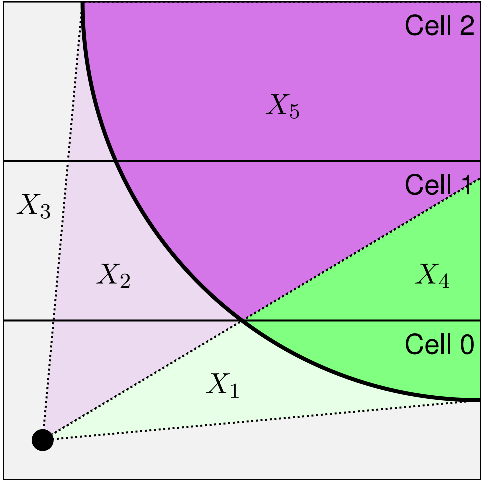

Combined Techniques: Governing Equation

- The combined-technique HSME has two possible steps, one with DXTRAN

$$
\begin{aligned}
\Psi_{FC,DX}(\boldsymbol{p}) = \mathcal{B}_c(\boldsymbol{p},\boldsymbol{p}_1)\mathcal{K}_A(\boldsymbol{p}_1,\boldsymbol{p}_2) \\
\times \left(\bar{s}_A(\boldsymbol{p}_1) + \mathcal{B}_t(\boldsymbol{p},\boldsymbol{p}_4)\mathcal{S}(\boldsymbol{p}_4,\boldsymbol{p}_5)(\bar{s}_S(\boldsymbol{p}_4) + \Psi_{FC,DX}(\boldsymbol{p}_5))\right) \\
+ \mathcal{B}_c(\boldsymbol{p},\boldsymbol{p}_1)\mathcal{K}_E(\boldsymbol{p}_1,\boldsymbol{p}_3) \\
\times \Big(\bar{s}_E(\boldsymbol{p}_1) + \Psi^{DX}_{FC,DX}(\boldsymbol{p}_3) + \mathcal{B}_{DX}(\boldsymbol{p}_1,\boldsymbol{p}_6)\Psi^{DX}_{FC,DX}(\boldsymbol{p}_6) \\
+ \mathcal{B}_t(\boldsymbol{p},\boldsymbol{p}_4)\mathcal{S}(\boldsymbol{p}_4,\boldsymbol{p}_5)(\bar{s}_S(\boldsymbol{p}_4) + \Psi_{FC,DX}(\boldsymbol{p}_5))\Big),\ \boldsymbol{p} \in \{\boldsymbol{p}_{FC}\}
\end{aligned}
\tag{15}
$$

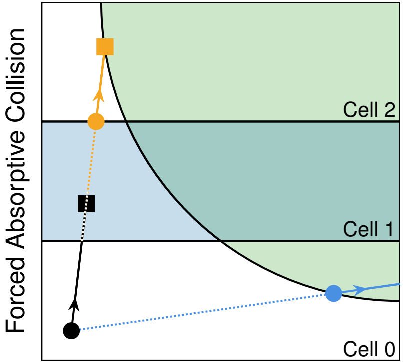

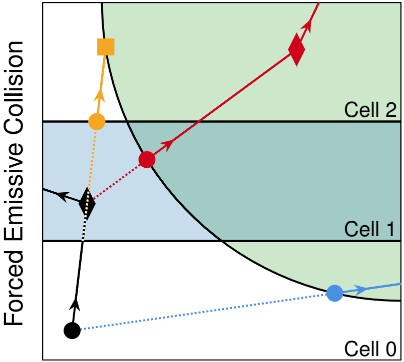

Combined Techniques: Equivalence to Analog Transport

- Can be rewritten as

$$\begin{aligned}\Psi_{FC,DX}(\boldsymbol{p}) &= \mathcal{B}_c(\boldsymbol{p},\boldsymbol{p}_1)\mathcal{K}_A(\boldsymbol{p}_1,\boldsymbol{p}_2)\bar{s}_A(\boldsymbol{p}_1) \\ &+ \mathcal{B}_c(\boldsymbol{p},\boldsymbol{p}_1)\mathcal{K}_E(\boldsymbol{p}_1,\boldsymbol{p}_3)\big(\bar{s}_E(\boldsymbol{p}_1) + \Psi^{DX}_{FC,DX}(\boldsymbol{p}_3)\big) \\ &+ \mathcal{B}_c(\boldsymbol{p},\boldsymbol{p}_1)(\mathcal{K}_A(\boldsymbol{p}_1,\boldsymbol{p}_2) + \mathcal{K}_E(\boldsymbol{p}_1,\boldsymbol{p}_3)) \\ &\times \mathcal{B}_t(\boldsymbol{p},\boldsymbol{p}_4)\mathcal{S}(\boldsymbol{p}_4,\boldsymbol{p}_5)(\bar{s}_S(\boldsymbol{p}_4) + \Psi_{FC,DX}(\boldsymbol{p}_5)) \\ &+ \mathcal{B}_c(\boldsymbol{p},\boldsymbol{p}_1)\mathcal{K}_E(\boldsymbol{p}_1,\boldsymbol{p}_3)\mathcal{B}_{DX}(\boldsymbol{p}_1,\boldsymbol{p}_6)\Psi^{DX}_{FC,DX}(\boldsymbol{p}_6),\ \boldsymbol{p} \in \{\boldsymbol{p}_{FC}\}\end{aligned} \tag{16}$$

- Looking at cases of streaming into either cell or DXTRAN surface shows

$$\mathcal{B}_c(\boldsymbol{p},\boldsymbol{p}_1) + w_c(\boldsymbol{p}) \to \mathcal{T}_{DX}(\boldsymbol{p},\boldsymbol{p}_1)$$

$$\mathcal{B}_t(\boldsymbol{p},\boldsymbol{p}_4) + w_t(\boldsymbol{p}) \to \mathcal{T}_{DX}(\boldsymbol{p},\boldsymbol{p}_4)$$

$$\mathcal{B}_c(\boldsymbol{p},\boldsymbol{p}_1)(\mathcal{K}_A(\boldsymbol{p}_1,\boldsymbol{p}_2) + \mathcal{K}_E(\boldsymbol{p}_1,\boldsymbol{p}_3)) = 1$$

- **Reducing forced-collision operators reveals DXTRAN behavior**

$$\boldsymbol{\Psi_{FC,DX}(p),\ p \in \{p_{FC}\} = \Psi_{DX}(p)}$$

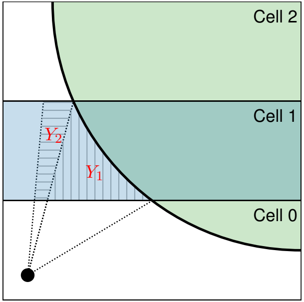

Proof of Fair Techniques Conclusions

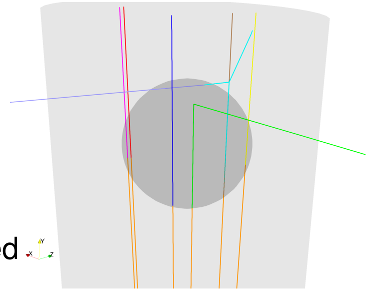

- Instigating case was inconsistent but unbiased
  - Forced-collision and DXTRAN techniques were correctly combined
  - Forced-collision was only applied to misidentified DXTRAN particles
  - Code change for consistency has been proposed
- All techniques are fair
  - Detailed report available after LA-UR
  - Assumptions underlying prior work [7] are not used
- DXTRAN can be played fairly on collision-by-collision basis
  - Analog transport after emergence was assumed and later replaced
  - Could also only apply technique at select emergence events
  - Applies to sequenced forced-flight regions in the MCBEND code [8, Sec. 2.4.2]

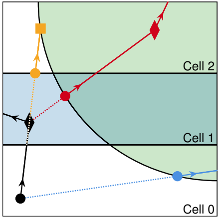

Derivation of the Integro-Differential Form of the Future Time Equation

Background on Monte Carlo Computational Time

- Future time: Computational time required to simulate a particle at $\boldsymbol{p}$ through a history
- Future Time Equation (FTE) is derived similarly to the HSME [9]
  - Future Time PDF (FTPDF) is derived with time required as response of interest
  - First time moment of FTPDF gives the FTE
  - Source terms are time required to process event (~ns)

$$\begin{aligned}\Upsilon(\boldsymbol{p}) = &\mathcal{T}(\boldsymbol{p},\boldsymbol{p}_1)\mathcal{K}_A(\boldsymbol{p}_1,\boldsymbol{p}_2)(\tau_{\text{trans}} + \tau_{\text{col},A}) \\ &+ \mathcal{T}(\boldsymbol{p},\boldsymbol{p}_1)\mathcal{K}_E(\boldsymbol{p}_1,\boldsymbol{p}_3)(\tau_{\text{trans}} + \tau_{\text{col},E} + \Upsilon(\boldsymbol{p}_3)) \\ &+ \mathcal{T}(\boldsymbol{p},\boldsymbol{p}_4)\mathcal{S}(\boldsymbol{p}_4,\boldsymbol{p}_5)(\tau_{\text{trans}} + \tau_{\text{surf}} + \Upsilon(\boldsymbol{p}_5))\end{aligned} \tag{17}$$

Motivation for Determining Expected Future Time

- Careful selection of VR parameters is used to optimize Monte Carlo codes
- Consistent Adjoint Driven Importance Sampling (CADIS) [10]
  - Determines VR parameters from adjoint function
  - Accelerates calculations through population control
  - Can lead to sub-optimal VR parameters due to oversplitting
- The solution of the FTE may be useful in addressing oversplitting
- Derivation of the integro-differential of the analog FTE is useful for:
  - Assisting future researchers understand the method
  - Being extended to include VR techniques
  - Providing a form conducive to a familiar deterministic solution

Future Time Equation Derivation Results

- Eq. 17 can be cast first into characteristic coordinates and then into an integro-differential form

$$
\begin{aligned}
&-\hat{\boldsymbol{\Omega}}\cdot\nabla\Upsilon(\boldsymbol{p})+\Sigma_t(\boldsymbol{x},E)\Upsilon(\boldsymbol{p})= \\
&\qquad\iint\Sigma_s(\boldsymbol{x},\hat{\boldsymbol{\Omega}}\rightarrow\hat{\boldsymbol{\Omega}}',E\rightarrow E')\Upsilon(\boldsymbol{x},\hat{\boldsymbol{\Omega}}',E',w)dE'd\Omega' \\
&\qquad\qquad+\Sigma_a(\boldsymbol{x},E)\left(\tau_{\text{trans}}+\tau_{\text{col},A}\right) \\
&\qquad\qquad\qquad+\Sigma_s(\boldsymbol{x},E)\left(\tau_{\text{trans}}+\tau_{\text{col},E}\right) \qquad (18a)
\end{aligned}
$$

where,

$$
\Upsilon(\boldsymbol{p})=\tau_{\text{trans}}+\tau_{\text{surf}}+\Upsilon_{\text{outside}}(\boldsymbol{p}),\ \boldsymbol{x}\in\delta\Gamma,\ \hat{\boldsymbol{\Omega}}\cdot\boldsymbol{n}>0 \qquad (18b)
$$

- Similar to the adjoint neutron transport equation with special source terms

Future Time Equation Solution Results

- After source terms are calculated, Eq. 18 can be solved with discrete ordinates methods [11]
- Material properties:
  - Air $\Sigma_t = 4.76 \times 10^{-4}$ cm^{-1}, $\Sigma_s = 0.920\Sigma_t$
  - Shield $\Sigma_t = 4.65$ cm^{-1}, $\Sigma_s = 0.063\Sigma_t$
  - Floor $\Sigma_t = 0.304$ cm^{-1}, $\Sigma_s = 0.975\Sigma_t$

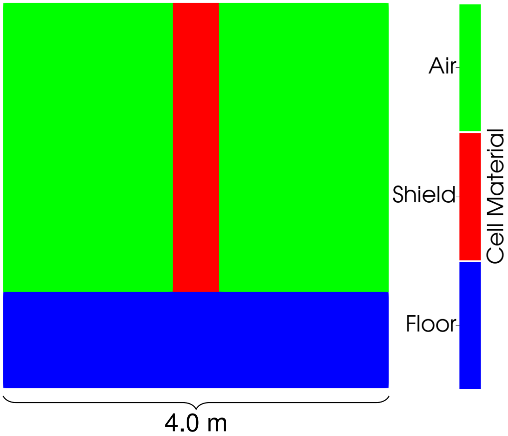

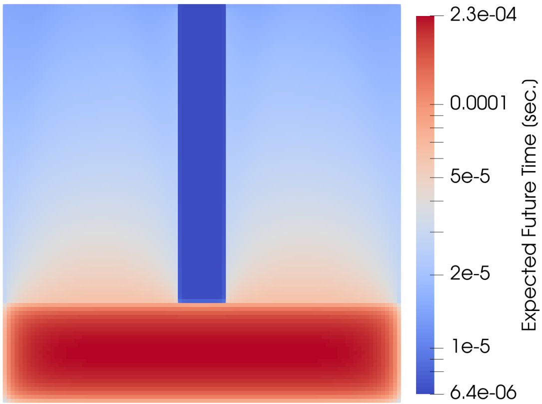

Integration of the LLNL Pulsed Sphere Benchmarks into V&V Framework

LLNL Pulsed Sphere V&V Suite Introduction

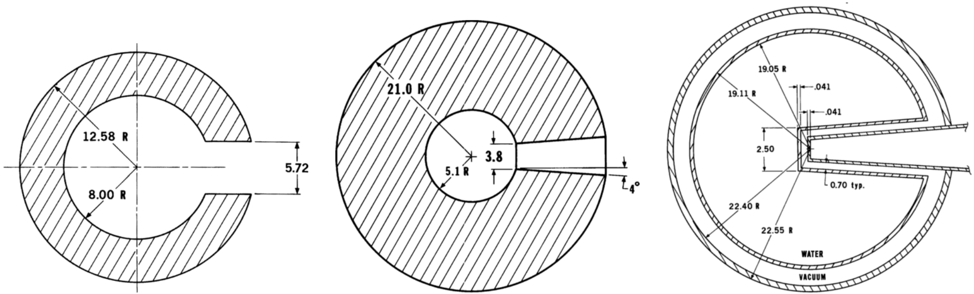

Geometry of beryllium, concrete, and water pulsed spheres [12].

- Time spectra were measured from spheres of various materials pulsed with 14-MeV neutrons during the Livermore Pulsed Sphere Program [12]
- Inputs replicating the Livermore Pulsed Sphere (LPS) experiments exist [5, 6]
- New V&V framework is being developed to automatically run simulations, compare results with experimental data, and produce documentation

LLNL Pulsed Sphere V&V Suite Results

- Select LPS inputs and experimental results have been integrated into the V&V framework
  - Materials: Beryllium, carbon, concrete, lithium-6, iron, and water
  - Models: A relatively simplistic legacy model and a more detailed model
  - Nuclear Data: ENDF/B-VI.6, ENDF/B-VII.0, ENDF/B-VII.1, and ENDF/B-VIII.0

0.1.3 Concrete

The time-of-flight spectra for a 2.0 MFP (14-MeV neutron) thick concrete pulsed sphere modeled with legacy and detailed CSG is given in Fig. 3. The legacy model has an average ratio of calculation to measured results of $1.0117 \pm 5.77\%$ and the detailed model has an average ratio of $0.9919 \pm 5.11\%$.

0.1.4 Iron

The time-of-flight spectra for a 0.9 MFP (14-MeV neutron) thick iron pulsed sphere modeled with legacy and detailed CSG is given in Fig. 4. The legacy model has an average ratio of calculation to measured results of $0.9743 \pm 5.71\%$ and the detailed model has an average ratio of $0.9451 \pm 4.23\%$.

0.1.5 Lithium-6

The time-of-flight spectra for a 1.6 MFP (14-MeV neutron) thick lithium-6 pulsed sphere modeled with legacy and detailed CSG is given in Fig. 5. The legacy model has an average ratio of calculation to measured results of $1.0974 \pm 5.97\%$ and the detailed model has an average ratio of $1.0917 \pm 5.38\%$.

0.1.6 Water

The time-of-flight spectra for a 1.9 MFP (14-MeV neutron) thick water pulsed sphere modeled with legacy and detailed CSG is given in Fig. 6. The legacy model has an average ratio of calculation to measured results of $1.0875 \pm 27.52\%$ and the detailed model has an average ratio of $1.0442 \pm 23.53\%$.

Note that the uncertainty in the average ratio of calculated to experimental time-of-flight results is calculated by propagating both the calculation result uncertainty and the experimental measurement uncertainty. From Fig. 6 one sees more measurement uncertainty compared to other materials, this is the cause of the high average ratio uncertainty for this material.

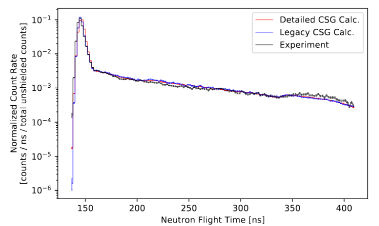

Figure 1: Comparison of the measured and calculated normalized count rate of neutrons escaping from a 0.8 MFP (14-MeV neutron) thick sphere of beryllium plotted against flight time.

Conclusions

Conclusions

- Variance-Reduction Fairness:
  - Forced-collision, DXTRAN, and combined techniques are fair
  - The MCNP code implements these techniques correctly
- Future Time Equation:
  - PDF $\rightarrow$ moment equation formalism is useful for different responses of interest
  - Integro-differential form of the FTE is very similar to the NTE
- LLNL Pulsed Spheres:
  - Have been incorporated into the V&V suite

Questions?

Contact information:

Email: peareric@lanl.gov (defunct 8/13/21)

Alternative email: peareric@umich.edu

References (1/3)

[1] R. J. Juzaitis, “Minimizing the Cost of Splitting in Monte Carlo Radiation Transport Simulation,” Ph.D. Thesis, University of Virginia, Oct. 1980, LA-8546-T. [Online]. Available: https://doi.org/10.2172/6753224

[2] C. J. Solomon, “Discrete-Ordinates Cost Optimization of Weight-Dependent Variance Reduction Techniques for Monte Carlo Neutral Particle Transport,” Ph.D. Thesis, Kansas State University, Dec. 2010. [Online]. Available: http://hdl.handle.net/2097/7014

[3] J. A. Kulesza, “Cost-optimized Automated Variance Reduction for Highly Angle-dependent Radiation Transport Analyses,” Ph.D. Thesis, University of Michigan, 2018. [Online]. Available: http://hdl.handle.net/2027.42/147541

[4] B. C. Kiedrowski, J. A. Kulesza, C. J. Solomon, “Discrete Ordinates Prediction of the Forced-Collision Variance Reduction Technique in Slab Geometry,” in *Proc. 2019 ANS Math. and Comp. Div.*, Aug. 2019.

[5] J. D. Court, R. C. Brockhoff, and J. S. Hendricks, “Lawrence Livermore Pulsed Sphere Benchmark Analysis of MCNP^{TM} ENDF/B-VI,” Los Alamos National Laboratory, Los Alamos, NM, USA, Tech. Rep. LA-12885, Dec. 1994. [Online]. Available: https://mcnp.lanl.gov/pdf_files/la-12885.pdf

References (2/3)

[6] J. A. Bucholz and S. C. Frankle, “Improving the LLNL Pulsed Sphere Experiments Database and MCNP Models,” Los Alamos National Laboratory, Los Alamos, NM, USA, Tech. Rep. LA-UR-03-3537, May 2003. [Online]. Available: https://mcnp.lanl.gov/pdf_files/la-ur-03-3537.pdf

[7] T. E. Booth and S. Pederson, “Unbiased Combinations of Nonanalog Monte Carlo Techniques and Fair Games,” *Progress in Nuclear Energy*, vol. 24, no. 1–3, pp. 21–25, 1990. [Online]. Available: https://doi.org/10.1016/0149-1970(90)90019-2

[8] P. Cowan, G. Dobson, and J. Martin, “Release of MCBEND 11,” *Progress in Nuclear Science and Technology*, vol. 4, pp. 437–440, 2014. [Online]. Available: https://doi.org/10.15669/pnst.4.437

[9] E. J. Pearson, J. A. Kulesza, and B. C. Kiedrowski, “Derivation of the Future Time Equation for Analog, Non-Multiplying Monte Carlo Simulation,” Los Alamos National Laboratory, Los Alamos, NM, US, Tech. Rep. LA-UR-21-25127, May 2021. [Online]. Available: https://doi.org/10.2172/1785476

References (3/3)

[10] J. C. Wagner, D. E. Peplow, and S. W. Mosher, “FW-CADIS Method for Global and Regional Variance Reduction of Monte Carlo Radiation Transport Calculations,” *Nuclear Science and Engineering*, vol. 176, no. 1, pp. 37–57, Jan. 2014. [Online]. Available: http://www.ans.org/pubs/journals/nse/a_35437

[11] E. J. Pearson, J. A. Kulesza, and B. C. Kiedrowski, “Discrete Ordinate Prediction of Analog Monte Carlo Computational Time with Embedded Timer Estimators,” *Trans. Am. Nucl. Soc.*, 2021, submitted.

[12] C. Wong, J. D. Anderson, P. Brown, L. F. Hansen, J. L. Kammerdiener, C. Logan, and B. Pohl, “Livermore Pulsed Sphere Progam: Program Summary through July 1971,” Lawerence Livermore National Laboratory, Livermore, CA, US, Tech. Rep. UCRL-51144, Rev. 1, Feb. 1972. [Online]. Available: https://mcnp.lanl.gov/pdf_files/ucrl-51144.pdf

Backup Slides

Combined Techniques Visualization

- Particles entering forced-collision cell (middle) are collided before reaching the DXTRAN sphere

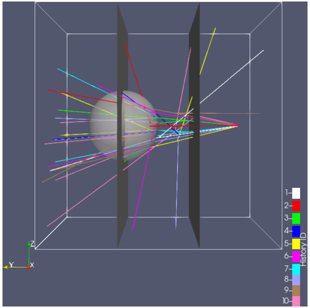

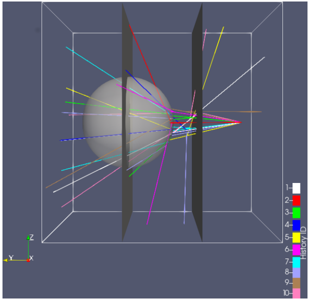

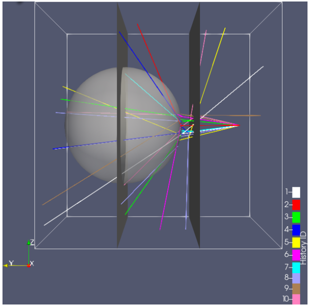

Abstract

To determine whether the combination of forced-collision and DXTRAN variance-reduction (VR) techniques is unbiased, and to gain insight into the operation of these techniques, proof that first-moment estimates from Monte Carlo simulations employing both techniques are unbiased is developed. A general background on the forced-collision and DXTRAN VR techniques and their combination is given. Proof of an unbiased simulation is outlined by showing the equivalence of the history score moment equations of simulations with these techniques in use. A report with detailed proof of this equivalence is available upon request. The derivation of the future time equation using a similar approach, as well as a summary of the addition of the LLNL Pulsed Sphere experiments to the MCNP verification and validation suite, is also briefly discussed.